

**$G^0W^0$  band gap of ZnO: Effects of plasmon-pole models**

M. Stankovski,<sup>1</sup> G. Antonius,<sup>1,2</sup> D. Waroquiers,<sup>1</sup> A. Miglio,<sup>1</sup> H. Dixit,<sup>3</sup> K. Sankaran,<sup>1</sup> M. Giantomassi,<sup>1</sup> X. Gonze,<sup>1</sup> M. Côté,<sup>2</sup> and G.-M. Rignanese<sup>1</sup>

<sup>1</sup>*Institut de la Matière Condensée et des Nanosciences (IMCN)-Nanoscopic Physics (NAPS), Université Catholique de Louvain, Place Croix du Sud 1, B-1348 Louvain-la-Neuve, Belgium*

<sup>2</sup>*Département de Physique, Université de Montréal, C.P. 6128, Succursale Centre-Ville, Montréal, Canada H3C 3J7*

<sup>3</sup>*Condensed Matter Theory (CMT)-Electron Microscopy for Materials Science (EMAT), Departement Fysica, Universiteit Antwerpen, Groenenborgerlaan 171, B-2020, Antwerpen, Belgium*

(Received 23 October 2011; published 5 December 2011)

Carefully converged calculations are performed for the band gap of ZnO within many-body perturbation theory ( $G^0W^0$  approximation). The results obtained using four different well-established plasmon-pole models are compared with those of explicit calculations without such models (the contour-deformation approach). This comparison shows that, surprisingly, plasmon-pole models depending on the  $f$ -sum rule gives less precise results. In particular, it confirms that the band gap of ZnO is underestimated in the  $G^0W^0$  approach as compared to experiment, contrary to the recent claim of Shih *et al.* [*Phys. Rev. Lett.* **105**, 146401 (2010)].

DOI: 10.1103/PhysRevB.84.241201

PACS number(s): 71.20.Nr, 31.15.vj, 71.15.Mb

Transparent conducting oxides (TCOs) are a class of technologically important materials for optoelectronic and spintronic applications.<sup>1</sup> Doped zinc oxide (ZnO) is among possible cheap alternatives to indium-based oxides which have generated considerable interest in the past decade.<sup>2</sup> From the theoretical standpoint, first-principles many-body calculations, which are now routinely used in order to make comparison with experiments, have proven surprisingly difficult even for pure bulk ZnO. The reported theoretical band gaps for the naturally occurring polymorph (the wurtzite structure) range from  $\sim 2.1$  eV to 4.2 eV,<sup>3–13</sup> to be compared with a measured value of 3.6 eV.<sup>14</sup> Recently, Shih *et al.*<sup>11</sup> claimed that a reasonable theoretical gap could be obtained by using conventional perturbative  $G^0W^0$  and including a Hubbard  $U$  parameter to account for the strongly correlated Coulomb repulsion between the Zn semicore  $d$  states and the valence shell  $p$  states. The implication of Ref. 11 is that all prior calculations have been underconverged due to a deceptive interrelationship between convergence parameters. In their work, Shih *et al.* used a plasmon-pole model (PPM) to account for the frequency dependence of the inverse dielectric function of the material. However, results can vary greatly depending on the exact PPM used.<sup>15,16</sup> In this Rapid Communication we study in great detail, and to a high numerical accuracy, exactly what effect different plasmon-pole models have on the value of the band gap. In order to compare our results closely with those of Ref. 11, we use the same numerical parameters,<sup>17</sup> and we also perform full-frequency calculations. We first introduce the theory of the PPM and full-frequency approaches. Then we present results for ZnO, and finally a discussion with a deeper analysis is provided. We show that the converged band gap strongly depends on the choice of plasmon-pole model, and that, without such a model, the  $G^0W^0$  approach fails to agree with experiment.

*Theory.* The application of perturbative quasiparticle (QP) corrections from a density functional theory (DFT) starting point is a long-standing success story in condensed-matter theory.<sup>23</sup> The central assumption is that Kohn-Sham (KS) orbitals are a good approximation to the QP orbitals, and

thus only a single iteration of Hedin's  $GW$  approximation<sup>24</sup> needs to be performed ( $G^0W^0$  approximation). A first-order correction to the KS eigenenergies is obtained through the Taylor expansion of the self-energy  $\Sigma(\omega)$  to first order around the KS energy eigenvalues. The self-energy is typically split as  $\Sigma(\omega) = \Sigma_x + \Sigma_c(\omega)$  into a frequency-independent pure-exchange part  $\Sigma_x$  and a correlation part evaluated as

$$\Sigma_c(\omega) = -i \int_{-\infty}^{\infty} d\omega' G(\omega + \omega') W^{\text{dyn}}(\omega'), \quad (1)$$

where we have suppressed the fact that the complex-valued  $\Sigma_c$ , Green's function  $G$ , and dynamic part of the screened interaction  $W^{\text{dyn}}$  are functions of two spatial coordinates.  $\Sigma_c$  and  $W^{\text{dyn}}$  obey Kramers-Kronig causality relations. In periodic crystalline systems, these quantities are expanded in a plane-wave basis, with  $\mathbf{G}, \mathbf{G}'$  labeling reciprocal-lattice vectors, and  $\mathbf{q}$  labeling a wave vector, giving

$$W_{\mathbf{G}, \mathbf{G}'}^{\text{dyn}}(\mathbf{q}, \omega) = [\epsilon_{\mathbf{G}, \mathbf{G}'}^{-1}(\mathbf{q}, \omega) - \delta_{\mathbf{G}, \mathbf{G}'}] v_{\mathbf{G}, \mathbf{G}'}(\mathbf{q}), \quad (2)$$

where  $\epsilon^{-1}$  is the inverse dielectric matrix calculated in the random-phase approximation with a sum over unoccupied states<sup>25,26</sup> and  $v$  the Coulomb potential (in matrix form). In principle, these matrices are infinite, but in practice they are zeroed beyond a maximum wave vector  $|\mathbf{q} + \mathbf{G}|$ , or energy  $\frac{1}{2}|\mathbf{q} + \mathbf{G}|^2$ . All plasmon-pole approximations enable an analytic solution of the convolution in Eq. (1) by positing a functional approximation to the frequency dependence in  $\epsilon^{-1}$ . The simplest possible approximation is the assumption that all the spectral weight in  $\text{Im}(\epsilon^{-1})$ , for positive frequencies, is concentrated in a single Dirac delta peak for each matrix element:

$$\begin{aligned} \text{Im}[\epsilon_{\mathbf{G}, \mathbf{G}'}^{-1}(\mathbf{q}, \omega)] &= A_{\mathbf{G}, \mathbf{G}'}(\mathbf{q}) \\ &\quad \times [\delta(\omega - \tilde{\omega}_{\mathbf{G}, \mathbf{G}'}(\mathbf{q})) - \delta(\omega + \tilde{\omega}_{\mathbf{G}, \mathbf{G}'}(\mathbf{q}))], \\ \text{Re}[\epsilon_{\mathbf{G}, \mathbf{G}'}^{-1}(\mathbf{q}, \omega)] &= \delta_{\mathbf{G}, \mathbf{G}'} + \frac{\Omega_{\mathbf{G}, \mathbf{G}'}^2(\mathbf{q})}{\omega^2 - \tilde{\omega}_{\mathbf{G}, \mathbf{G}'}^2(\mathbf{q})}, \end{aligned} \quad (3)$$

where the  $\mathbf{G}, \mathbf{G}'$  and  $\mathbf{q}$ -dependent weight of the delta peak  $A$ , oscillator strength  $\Omega$ , and pole position  $\tilde{\omega}$  are to be determined.

Two of these parameters are independent, and the third can be found through the Kramers-Kronig relation. PPMs were originally introduced by Hedin<sup>27</sup> for the homogenous electron gas and then generalized for arbitrary crystalline systems by Hybertsen and Louie (HL),<sup>28</sup> and also by Godby and Needs (GN).<sup>29</sup> The HL PPM fixes the dependence of the pole position and the oscillator strength by requiring that the plasmon-pole parameters reproduce the value of  $\epsilon^{-1}$  in the static limit ( $\omega = 0^+$ ), as well as fulfilling Johnson's frequency sum ( $f$ -sum) rule<sup>30</sup>

$$\int_0^\infty d\omega \omega \text{Im}[\epsilon_{\mathbf{G},\mathbf{G}'}^{-1}(\mathbf{q},\omega)] = 2\pi^2 \frac{(\mathbf{q}+\mathbf{G})(\mathbf{q}+\mathbf{G}')}{|\mathbf{q}+\mathbf{G}|^2} n_{\mathbf{G}-\mathbf{G}'}, \quad (4)$$

where  $n_{\mathbf{G}-\mathbf{G}'}$  is the electron density in reciprocal space. In this way the low and high real frequency limits are exact, and the PPM only requires the dielectric function to be explicitly evaluated at  $\omega = 0^+$ . In contrast, the GN PPM takes advantage of analytic continuation into the complex plane  $\epsilon^{-1}(\omega) \rightarrow \epsilon^{-1}(i\omega)$  and determines the parameters through the explicit evaluation of the dielectric function for a second point along the imaginary frequency axis, typically taken to be near the real plasma frequency of the system if known, or near the plasma frequency as evaluated from the average density per volume  $i\omega_p = i\sqrt{4\pi n_0}$ .

For comparison, the models of von der Linden and Horsch<sup>31</sup> (vdLH) and Engel and Farid<sup>32</sup> (EF) have also been tested in this work. They are both based on the spectral decomposition of the symmetrized dielectric matrix, and use the zero-frequency limit and the  $f$ -sum rule to fix the parameters.

If a PPM is to be avoided, the frequency convolution in Eq. (1) needs to be performed numerically. However, the poles of the Kohn-Sham Green's function are right on the axis, and so the spectral function has a long—in principle, infinite—set of very sharp peaks there. It is then more convenient to recast the integral in Eq. (1) with the use of an appropriate contour in the complex plane as

$$\begin{aligned} \Sigma_c(\omega) &= - \sum_s^{\mathcal{C}} \lim_{z \rightarrow z_s} G(z_s) W^{\text{dyn}}(z_s)(z - z_s) \\ &\quad - \frac{i}{2\pi} \int_0^\infty d(i\omega') G(\omega + i\omega') W^{\text{dyn}}(i\omega') \quad (5) \\ &= - \sum_{\mathbf{q}}^{\text{BZ}} \sum_s^{\mathcal{C}} \mathcal{M}_{\mathbf{G},\mathbf{G}'}^s(\mathbf{k},\mathbf{q}) \left\{ W_{\mathbf{G},\mathbf{G}'}^{\text{dyn}}(\mathbf{q},|\omega - \varepsilon_s| - i0^+) \right. \\ &\quad \times [\theta(\omega - \varepsilon_s)\theta(\varepsilon_s - \mu) - \theta(\varepsilon_s - \omega)\theta(\mu - \varepsilon_s)] \\ &\quad \left. + 2i \int_0^\infty d(i\omega') \frac{(\omega - \varepsilon_s)}{(\omega - \varepsilon_s)^2 + \omega'^2} W_{\mathbf{G},\mathbf{G}'}^{\text{dyn}}(\mathbf{q},i\omega') \right\}, \quad (6) \end{aligned}$$

where Eq. (5) is the general expression, while Eq. (6) is the special case of periodic systems  $\Sigma_c(\omega) \rightarrow \Sigma_{c\mathbf{G},\mathbf{G}'}(\mathbf{k},\omega)$  when the Green's function is constructed from Kohn-Sham (KS) orbitals with eigenvalues  $\varepsilon_s$ .  $\mathcal{M}$  is a frequency-independent function related to the oscillator matrix elements. The contour  $\mathcal{C}$  in the complex plane is described in detail in Ref. 33. The first term is the sum over poles enclosed in the contour, and, together with  $\Sigma_x$ , it forms the screened exchange part, while the second component with the integrated term is the so-called Coulomb-hole contribution. In practice, there is always a limit

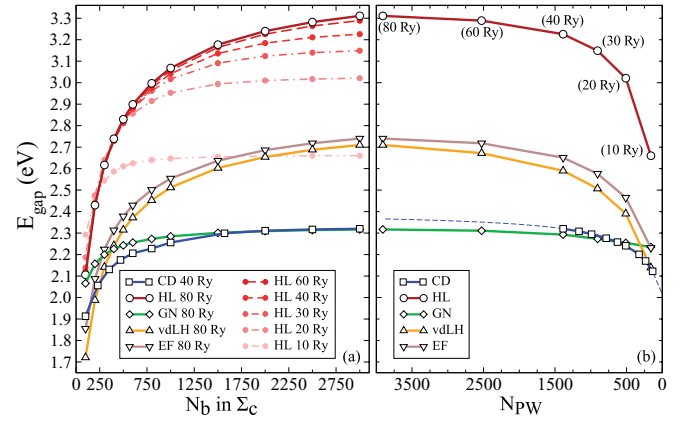


FIG. 1. (Color online) (a) Convergence of the LDA +  $G^0W^0$  band gap vs the number of bands included in the sum over unoccupied bands in the self-energy, and (b) convergence of the band gap vs the energy cutoff of the dielectric matrix. Contour deformation (CD) is the actual result, i.e., using a full-frequency treatment *without* a plasmon-pole model (PPM). The Hybertsen-Louie (HL), Godby-Needs (GN), von der Linden–Horsch (vdLH), and Engel-Farid (EF) PPMs (Ref. 17) seek to emulate the CD result. The CD curve in (a) is taken at 40 Ry, whereas the result at 80 Ry is expected to be where the extrapolated (Ref. 12) CD curve (squares) in (b) levels out.

to the total number of unoccupied states or bands  $N_b$  that can be included in the evaluation of the self-energy and in the screened interaction.

**Results for ZnO.** The QP corrections are calculated using the local density approximation<sup>34</sup> (LDA) of DFT as the starting point. To ease the comparison, we use the same computational parameters<sup>17</sup> as in Ref. 11. When the HL PPM is adopted, we reproduce the convergence behavior reported by Shih *et al.* [see Fig. 1(a)] for the  $G^0W^0$  band gap. However, when the other PPMs are used, the gap obtained is significantly lower. The convergence behaviors of the vdLH PPM and the EF PPM are similar to that of the HL PPM, i.e., there is a very slow convergence with respect to the number of bands and the plane-wave cutoff. For the GN PPM this behavior is milder, and  $\sim 800$  unoccupied bands (and a plane-wave cutoff of  $\sim 40$  Ry) is sufficient to converge the value of the gap to within 0.02 eV. The model-free contour deformation (CD) result has a slightly slower convergence rate than the GN PPM, with  $\sim 1700$  unoccupied bands being sufficient to converge. Clearly, the PPM which best reproduces the CD result is the GN PPM. To investigate the reasons for this, we have compared the behavior of  $\text{Re}[\epsilon^{-1}]$  for the GN and HL PPM with the actual one along both the imaginary and real axis. Some representative results for diagonal elements of  $\text{Re}[\epsilon^{-1}]$  (for  $\mathbf{q} = 0$ ) are shown in Figs. 2(a)–2(l).

It is clear that both PPMs are crude approximations, even though they match at the zero-frequency limit. However, the HL PPM has its weight fixed by the sum rule, and this forces the pole position ever further out on the real axis. In turn, this seems to create an overestimation of the contribution from the pole along the imaginary axis, especially in the low-frequency region. Here, the GN PPM is a much better match due to its construction as a minimal pole fit along the imaginary axis.

Since all PPMs which use the  $f$ -sum rule to fix the pole parameters lead to a systematic overestimation of the gap, it

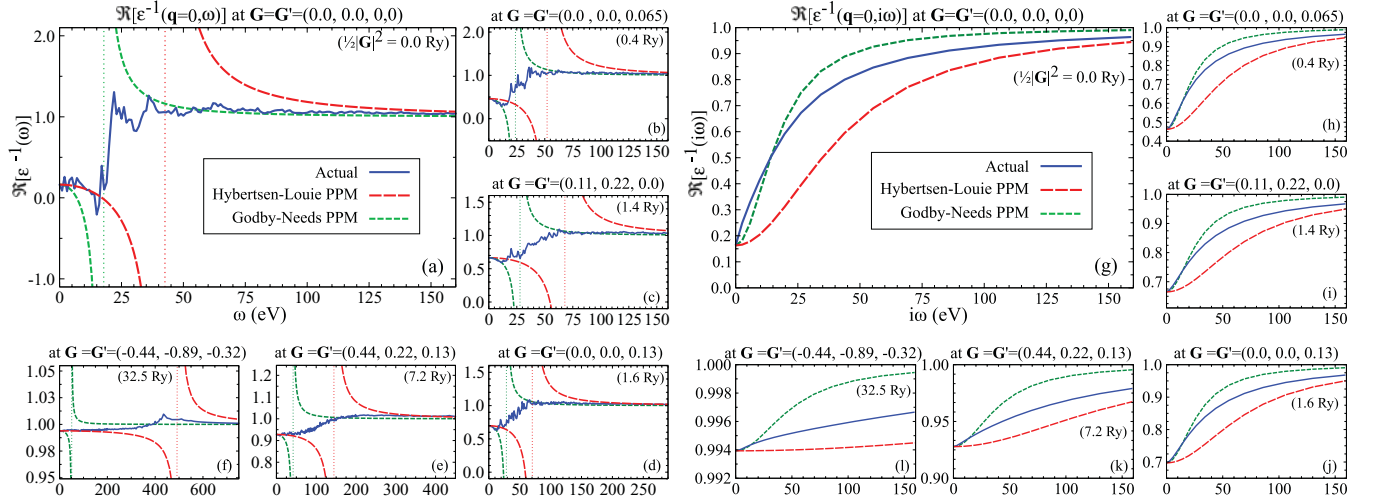


FIG. 2. (Color online) Examples of the actual  $\text{Re}[\epsilon^{-1}]$  along the real [(a)–(f)] and imaginary [(g)–(l)] axis for some diagonal matrix elements ( $\frac{1}{2}|\mathbf{G}|^2$  is given in parentheses in each plot) compared to that of the PPMs. The full (blue/dark gray) line is the actual function, the (red/light gray) line with long dashes is the HL PPM, and the (green/light gray) short dashed line is the GN PPM. The pole position on the real axis is indicated by the vertical lines. The x and y axis labels of (a) apply to (b)–(f) and those of (g) to (h)–(l).

is interesting to estimate the importance of the fulfillment of this rule in the screening. As can be seen in Fig. 3(b), the sum rule is actually very poorly fulfilled by the GN PPM; it is by construction exactly fulfilled by the HL PPM, while for the model-free  $\epsilon^{-1}$ , its fulfillment is slowly achieved as more unoccupied states are added. The CD gap, however, is already converged with  $\sim 1000$  bands in the screening,

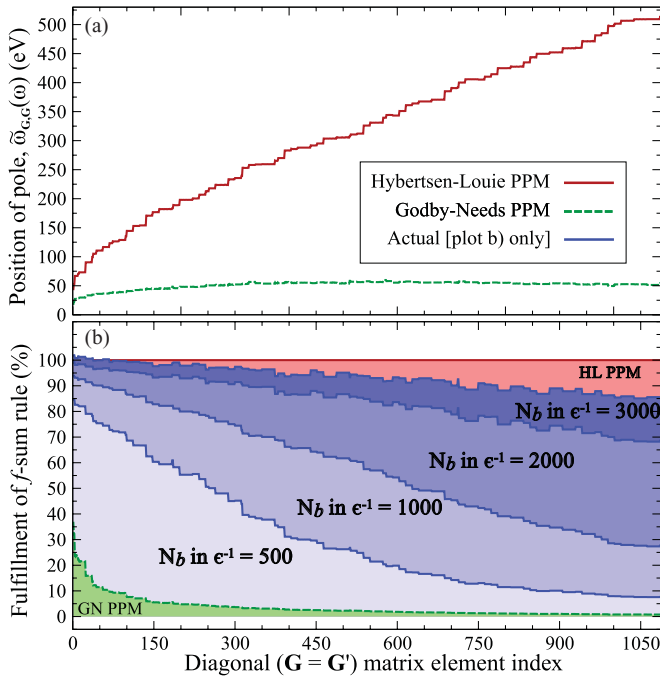


FIG. 3. (Color online) (a) The position of the GN and HL PPM pole for the diagonal elements of  $\epsilon^{-1}$  [where the vertical lines are in Figs. 2(a)–2(f)]. (b) The fulfillment of the  $f$ -sum per diagonal matrix element for the GN and HL PPMs. The blue/dark gray curves are the parameter-free results for various cutoffs of the number of unoccupied states included in the screening.

hence *fulfillment of the sum rule does not seem to be a critical criterion*, at least for most of the matrix elements of the dielectric function. Indeed, it seems that for a simple plasmon-pole model of the type defined in Eq. (3), it is very difficult to satisfy both a good overall match for the low-frequency region and a fulfillment of the sum rule. We have also checked the convergence with the  $k$ -point grid, as displayed in Table I. These results were done with a plane-wave cutoff of 80 Ry and the equivalent of  $\gtrsim 3000$  bands<sup>21</sup> included in both the screening and the self-energy. For the HL PPM, the value at  $5 \times 5 \times 4$  in the table is 0.2 eV higher than the most converged value in Fig. 1, indicating that the latter is still not entirely converged, as pointed out in Ref. 11. For the GN PPM, our best value is 2.35 eV. Based on Fig. 1 we expect that the corresponding CD value would be  $\sim 2.4$  eV. This is  $\sim 0.4$  eV lower than the value of 2.83 eV from the all-electron calculation of Friedrich *et al.*<sup>12</sup> The discrepancy should be entirely due to pseudoization and core-relaxation effects.<sup>35</sup> It is apparent that the LDA was never a good starting point, since the ground-state band gap of ZnO (0.67 eV in this work) is underestimated by as much as 80% and the RPA dielectric constant ( $\epsilon_\infty = 5.45$  in this work) is overestimated by  $\sim 44\%$  compared to experiment. The inclusion of a Hubbard  $U$  parameter (as used by Shih *et al.*) is not expected to remedy this, since it only leads to an opening of the ground-state and  $G^0W^0$  gaps of  $\sim 0.2$  eV.

TABLE I. ZnO LDA +  $G^0W^0$  gap (eV) convergence with respect to  $k$ -point grid, with the equivalent of  $\gtrsim 3000$  bands [through Bruneval-Gonze extrapolation (Ref. 21)] in the sums for  $W^{\text{dyn}}$  and  $\Sigma_c$  at a plane-wave cutoff of 80 Ry.

MP grid	$2 \times 2 \times 2$	$4 \times 4 \times 3$	$5 \times 5 \times 4$	$7 \times 7 \times 4$	$8 \times 8 \times 5$
HL PPM	3.448	3.571	3.559	3.574	3.566
GN PPM	2.215	2.351	2.344	2.363	2.352

*Discussion.* *A priori*, it makes perfect sense theoretically to fix the parameters of a single pole by using the  $f$ -sum rule, thus fixing the asymptotic high-frequency limit of the analytic pole approximation. However, our results show that this is inadvisable in the case of ZnO, and probably in many other cases where there is a strong influence of semicore states.<sup>15,16</sup> It is clear that a simple pole on the real axis is a very crude approximation to the true behavior of the screening, in fact, it seems surprising that it has worked so well thus far. The first problem is that a realistic crystalline solid actually has a whole plasmonic band-structure spectrum, and while a simple pole is a good approximation for the homogenous electron gas, in reality there are numerous plasma resonances depending on the crystal potential and the various electronic shells of the atomic cores. When it is necessary to take into account semicore states,<sup>13</sup> the valence density will be sharply peaked around the atomic cores, which leads to large and highly oscillatory values for very large  $\mathbf{G}, \mathbf{G}'$  components of the valence density in reciprocal space  $n_{\mathbf{G}-\mathbf{G}'}$ . This should account for the very slow convergence with respect to the plane-wave cutoff for all PPMs that employ the  $f$ -sum rule, a behavior which is absent when using the CD method or the GN PPM.

It is also surprising that the GN PPM works so well, given that it is based on exactly the same analytic form as the HL PPM. The reason for this is clear from an inspection of Eq. (6), where the sum over the poles of the Green's function, i.e., the dynamic screened exchange contribution, has restrictions on it imposed by the Heaviside functions. Only a very small range along the real-frequency axis is needed for the evaluation of the QP corrections for the states forming the gap (for ZnO, this range is  $\sim 0-1.1$  eV). As can be seen in Figs. 2(a)–2(f) (left section), for small frequencies both the GN and HL PPMs are decent approximations, for a large range of the plane-wave index. However, the Coulomb-hole contribution is given by the integration of the smooth functional behavior

of  $\epsilon^{-1}$  along the imaginary axis, multiplied by a Lorentzian centered at the origin. When  $\Sigma_c$  is evaluated at energies close to a KS eigenvalue, the Lorentzian will effectively become a delta function for a single term, and will be picking out the zero-frequency limit, which is also exactly fulfilled by all PPMs. Thus we know that the nonresonant terms in the Coulomb-hole contribution must become important, precisely for those materials where the GN and HL PPMs give a very different result. These terms probe the low-frequency region of  $W$  on the imaginary axis, and it is exactly here that the GN PPM is a much better approximation, while the contribution from the HL PPM is far too large due to the enforced  $f$ -sum rule. This difference is apparent in Figs. 2(g)–2(j) (right section). The GN approach is computationally more demanding, requiring two explicit evaluations of  $\epsilon^{-1}$  rather than one, but the added effort is not prohibitive on modern computers and well worth it for the added accuracy. In conclusion, ZnO is still an example of a system where one has to be careful about the choice of PPM, and the LDA +  $G^0W^0$  approach fails.

The authors would like to thank P. Zhang, S. Louie, J. Deslippe, P. Rinke, H. Jiang, C. Friedrich, and F. Bruneval for many helpful discussions. We are also very grateful to Y. Pouillon, A. Jacques, and J.-M. Beuken for their technical aid and expertise. M.C. and G.A. would like to acknowledge the support of NSERC and FQRNT. This work was supported by the Interuniversity Attraction Poles program (P6/42)–Belgian State–Belgian Science Policy, the Flemish Science Foundation (FWO-VI) ISIMADE project, the EU's 7th Framework programme through the ETSF I3 e-Infrastructure project (Grant Agreement No. 211956), the Communauté française de Belgique, through the Action de Recherche Concertée 07/12-003 “Nanosystèmes hybrides métal-organiques”, and the FNRS through FRFC Project No. 2.4.589.09.F.

<sup>1</sup>Ü. Özgür, Ya. I. Alivov, C. Liu, A. Teke, M. A. Reshchikov, S. Dogan, V. Avrutin, S.-J. Cho, and H. Morkoç, *J. Appl. Phys.* **98**, 041301 (2005).

<sup>2</sup>H. Hosono, *Thin Solid Films* **515**, 6000 (2007).

<sup>3</sup>S. Massidda, R. Resta, M. Posternak, and A. Baldereschi, *Phys. Rev. B* **52**, R16977 (1995).

<sup>4</sup>M. Usuda, N. Hamada, T. Kotani, and M. van Schilfgaarde, *Phys. Rev. B* **66**, 125101 (2002).

<sup>5</sup>A. R. H. Preston, B. J. Ruck, L. F. J. Piper, A. DeMasi, K. E. Smith, A. Schleife, F. Fuchs, F. Bechstedt, J. Chai, and S. M. Durbin, *Rev. B* **78**, 155114 (2008).

<sup>6</sup>A. Schleife, C. Rödl, F. Fuchs, J. Furthmüller, F. Bechstedt, P. H. Jefferson, T. D. Veal, C. F. McConville, L. F. J. Piper, A. DeMasi, K. E. Smith, H. Lössch, R. Goldhahn, C. Cobet, J. Zúñiga-Pérez, and V. Muñoz-Sanjose, *J. Korean Phys. Soc.* **53**, 2811 (2008).

<sup>7</sup>T. Kotani, M. van Schilfgaarde, and S. V. Faleev, *Phys. Rev. B* **76**, 165106 (2007).

<sup>8</sup>M. Shishkin and G. Kresse, *Phys. Rev. B* **75**, 235102 (2007).

<sup>9</sup>F. Fuchs, J. Furthmüller, F. Bechstedt, M. Shishkin, and G. Kresse, *Phys. Rev. B* **76**, 115109 (2007).

<sup>10</sup>Paola Gori, M. Rakel, C. Cobet, W. Richter, N. Esser, A. Hoffmann, R. Del Sole, A. Criscenti, and O. Pulci, *Phys. Rev. B* **81**, 125207 (2010).

<sup>11</sup>B.-C. Shih, Y. Xue, P. Zhang, M. L. Cohen, and S. G. Louie, *Phys. Rev. Lett.* **105**, 146401 (2010).

<sup>12</sup>C. Friedrich, M. C. Müller, and S. Blügel, *Phys. Rev. B* **83**, 081101(R) (2011).

<sup>13</sup>H. Dixit, R. Saniz, D. Lamoén, and B. Partoens, *J. Phys. Condens. Matter* **22**, 125505 (2010).

<sup>14</sup>S. Tsoi, X. Lu, A. K. Ramdas, H. Alawadhi, M. Grimsditch, M. Cardona, and R. Lauck, *Phys. Rev. B* **74**, 165203 (2006).

<sup>15</sup>R. Shaltaf, G.-M. Rignanese, X. Gonze, F. Giustino, and A. Pasquarello, *Phys. Rev. Lett.* **100**, 186401 (2008).

<sup>16</sup>W. Kang and M. S. Hybertsen, *Phys. Rev. B* **82**, 085203 (2010).

<sup>17</sup>The experimental structural parameters given in Ref. 18 are adopted for wurtzite ZnO. Where not otherwise specified, a  $5 \times 5 \times 4$  Monkhorst-Pack (Ref. 19) (MP) grid is used. All MP grids are shifted by (0.0,0.0,0.5) in reduced coordinates for the calculation of  $W^{\text{dyn}}$ , and  $\Gamma$  centered for  $\Sigma_c$ . The norm-conserving (Ref. 20) pseudopotentials are generated using the following atomic valence



configurations: Zn( $3s^2 3p^6 3d^{10} 4s^2$ ) and O( $2s^2 2p^4$ ). For Zn, a core radius of  $r_c = 0.42 \text{ \AA}$  is taken for all the waves and scalar-relativistic effects are included explicitly. For O, we use a  $r_c = 0.64 \text{ \AA}$  for both  $s$  and  $p$  waves. The plane-wave cutoff was 300 Ry for the wave functions, density, and  $\Sigma_x$ . For the results in Figs. 1 and 2,  $N_b = 1000$  in  $W^{\text{dyn}}$ . A broadening of 0.1 eV was used in the screening for the parameter-free results, below which convergence studies show a dependence of less than 0.05 eV of the gap. For the results in Table I, the extrapolar method was used (Ref. 21). All calculations made with ABINIT (Ref. 22).

- <sup>18</sup>K. Kihara and G. Donnay, *Can. Mineral.* **23**, 647 (1985).  
<sup>19</sup>H. J. Monkhorst and J. D. Pack, *Phys. Rev. B* **13**, 5188 (1976).  
<sup>20</sup>N. Troullier and J. L. Martins, *Phys. Rev. B* **43**, 1993 (1991).  
<sup>21</sup>We used the extrapolar method with 500 bands and an optimum convergence parameter, determined by convergence studies to be equivalent to the use of at least 3000 bands [F. Bruneval and X. Gonze, *Phys. Rev. B* **78**, 085125 (2008)].  
<sup>22</sup>X. Gonze *et al.*, *Comput. Phys. Commun.* **180**, 2582 (2009).

- <sup>23</sup>W. G. Aulbur, L. Jonsson, and J. W. Wilkins, *Solid State Phys.* **54**, 1 (2000).  
<sup>24</sup>L. Hedin and S. Lundqvist, in *Solid State Physics*, edited by H. Ehrenreich, F. Seitz, and D. Turnbull, Vol. 23 (Academic, New York, 1969), p. 1.  
<sup>25</sup>S. L. Adler, *Phys. Rev.* **126**, 413 (1962).  
<sup>26</sup>N. Wiser, *Phys. Rev.* **129**, 62 (1963).  
<sup>27</sup>L. Hedin, *Phys. Rev.* **139**, A796 (1965).  
<sup>28</sup>M. S. Hybertsen and S. G. Louie, *Phys. Rev. B* **34**, 5390 (1986).  
<sup>29</sup>R. W. Godby and R. J. Needs, *Phys. Rev. Lett.* **62**, 1169 (1989).  
<sup>30</sup>D. L. Johnson, *Phys. Rev. B* **9**, 4475 (1974).  
<sup>31</sup>W. von der Linden and P. Horsch, *Phys. Rev. B* **37**, 8351 (1988).  
<sup>32</sup>G. E. Engel and B. Farid, *Phys. Rev. B* **47**, 15931 (1993).  
<sup>33</sup>M. Giantomassi, M. Stankovski, R. Shaltaf, M. Grüning, F. Bruneval, P. Rinke, and G.-M. Rignanese, *Phys. Status Solidi B* **248**, 275 (2011).  
<sup>34</sup>J. P. Perdew and A. Zunger, *Phys. Rev. B* **23**, 5048 (1981).  
<sup>35</sup>R. Gómez-Abal, X. Li, M. Scheffler, and C. Ambrosch-Draxl, *Phys. Rev. Lett.* **101**, 106404 (2008).